Proceedings of the 8th World Congress on Mechanical, Chemical, and Material Engineering (MCM'22)
Prague, Czech Republic – July 31, 2022 - August 02, 2022
Paper No. HTFF 143
DOI: 10.11159/htff22.143

The Effect of Outlet Manifold Location of Liquid-Cooled Battery Thermal Management Systems on Pumping Power

Kuuku-Dadzie Botchway, Mohammad Reza Shaeri
Department of Mechanical Engineering, University of the District of Columbia, Washington, DC 20008 USA
kuuku.botchway@udc.edu; mohammadreza.shaeri@udc.edu

Abstract **–** Hydrothermal performances of two water-cooled thermal management systems (TMSs) for cooling lithium-ion batteries (LIBs) are compared through three-dimensional simulations of laminar flow and heat transfer in TMSs, as well as conduction heat transfer with volumetric heat generation inside the battery cell. Maximum cell temperature and temperature variation across the cell are used to evaluate thermal performances of TMSs. The TMSs are different from each other by location of outlet manifold. In the bottom outlet (BO) design, the outlet is located at the bottom of the TMS's case, while in the middle outlet (MO) design, the outlet manifold is located at the middle of the TMS's case. Both designs provide safe operational temperature for LIBs, although the thermal performance of BO design is slightly higher than that of the MO design. This is due to distribution of water over a larger surface area in the BO TMS compared with the MO TMS. To provide a better insight on practical applications of TMSs, their thermal performances are described based on pumping power. Due to a shorter path from the inlet to the outlet in the MO design, compared with the BO design, the pressure drop is lower in the MO TMS. As a result, at a given flow rate, the MO TMS operates with a lower pumping power compared with the BO TMS. The present study suggests that selecting an appropriate TMS highly depends on design priorities. If the main goal is to maintain the cell temperature as low as possible, the BO design is an effective TMS. If the design goal is to minimize the pumping power, the MO TMS is an effective cooling system.

Keywords**:** Thermal management; Lithium-ion battery; Liquid-cooled system; Pumping power; CFD.

1. Introduction

Performances of lithium-ion batteries (LIBs) as the main power sources for electric vehicles (EVs) strongly depend on the operating temperature of the batteries. An effective thermal management system (TMS) should maintain the temperature of battery cell within 20-50°C with less than 5°C of the temperature variation across the cell [1, 2]. However, in addition to providing a safe operating temperature for the battery cell, the TMS should operate with a minimized pumping power. Pumping power is a key design parameter in an active cooling system. A large pumping power may hinder using the cooling system regardless of its effective thermal performance [3]. In the present study, hydrothermal performances of two TMSs are compared. To provide a better insight on practical applications of TMSs, their thermal performances are described based on their pumping power. Fig. 1 illustrates the schematic of the two TMSs.

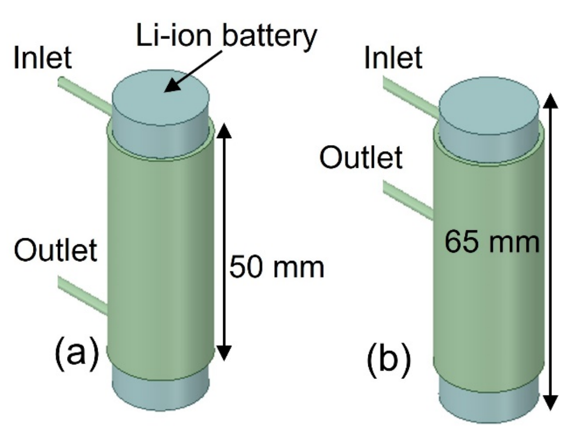

Fig. 1: Three-dimensional view of: (a) bottom outlet (BO) TMS; (b) middle outlet (MO) TMS.

The TMS is a cylindrical shell. Water, as the coolant, flows through the annulus with a thickness of 1 mm (i.e., the inner and outer diameters of the annulus are 18 mm and 20 mm, respectively). The thickness of the TMS's case is assumed zero. The diameter and height of the cylindrical LIB cell are 18 mm and 65 mm, respectively. The cell has a specific heat, thermal conductivity, and density of 1027 $J.kg^{-1}.K^{-1}$, 25 $W.m^{-1}.K^{-1}$, and 4035 $kg.m^{-3}$, respectively [4]. The TMS has a length of 50 mm and covers the LIB cell. From both sides of the LIB cell, a height of 7.5 mm is outside the TMS's case and exposed to the air. In both designs, the inlet is located at the top of the TMS's case. The difference between the TMSs is the location of the outlet manifold. In the bottom outlet (BO) design, the outlet is located at the bottom of the case, while in the middle outlet (MO) design, the outlet is located at the middle of the TMS's case. The diameter of inlet and outlet manifolds are 2 mm in both designs. Water at 22°C enters the inlet and exits the outlet. The simulations are performed at two volume flow rates of 0.1 and 0.2 LPM (liter/min). The maximum Reynolds number based on the hydraulic diameter of the annulus is ~ 2100, which indicates a laminar flow for all flow rates in the simulations. The governing equations to simulate the flow and heat transfer by assumption of a laminar, steady, and incompressible flow, as well as the constant properties for both the fluid and LIB cell are as follows:

Continuity:
$$\nabla . \boldsymbol{u} = 0 \tag{1}$$
Momentum conservation:
$$(\boldsymbol{u}. \nabla)\rho \boldsymbol{u} = -\nabla p + \mu \nabla^2 \boldsymbol{u} \tag{2}$$
Energy conservation (fluid):
$$\boldsymbol{u}. \nabla T_f = \frac{\lambda}{\rho c_p} \nabla^2 T_f \tag{3}$$
Energy conservation (solid):
$$k \nabla^2 T_s + \dot{q} = 0 \tag{4}$$

where ρ, u, p, μ, λ, c_p, and T_f are the fluid density, velocity, pressure, viscosity, thermal conductivity, specific heat, and temperature, respectively. k and T_s are the thermal conductivity and temperature of solid, respectively. Also, $\dot{q}$ is the volumetric heat generation in the battery cell. In this study, a constant value of $300\ \mathrm{KW.m^{-3}}$ is considered for $\dot{q}$, which corresponds to the critical condition at large discharge rates of LIBs [5]. Water flow rate and temperature are set at the inlet. Zero axial gradients for all the variables are imposed at the outlet. The remaining surfaces are walls with a no-slip boundary condition. All surfaces of the TMS and LIB that are exposed to the air are adiabatic. The temperature distribution on the interface of the solid and fluid is obtained by simultaneously solving the conjugate problem of heat conduction equation with convection in the fluid. A grid structure with 204,000 elements has been selected through grid independence tests, because by increasing the number of elements beyond 204,000, the magnitudes of heat transfer coefficients and friction coefficients changed negligibly. The governing equations are solved using Ansys Fluent.

2. Results

In this study, thermal performances of TMSs are represented by the maximum temperature of the LIB cell ($T_{\max}$) and the temperature difference across the cell (ΔT), and are described based on the pumping power (P_p) that is calculated as follows [6]:

$$P_p = \dot{V} \times \Delta P \tag{5}$$

where $\dot{V}$ and ΔP are the total volumetric flow rate and the pressure drop across the TMS, respectively. $T_{\max}$ and ΔT at different pumping powers are illustrated in Fig. 2. For a given TMS, reduction in the $T_{\max}$ by increasing the flow rate is due to the increased sensible heat. Although both TMSs maintain $T_{\max}$ and ΔT within the safe range of operational temperature, the BO design results in both lower $T_{\max}$ and ΔT at a given flow rate. This is most likely due to distribution of water over a larger surface (i.e., the zone between the inlet and outlet) inside the TMS's case in the BO design compared with the MO design. Fig. 3 compares the temperature distribution on the exterior surface of the LIB cell obtained from different TMSs at this study. Due to the location of the outlet at the middle of the TMS's case in MO design, flow distribution is different from the top half and bottom half of the TMS's case; as a result, hotter zones are created in the bottom half of MO TMS.

However, at a given flow rate, the MO design results in a lower pumping power compared with the BO TMS. This is is most likely due to flowing the liquid through a shorter path from the inlet to the outlet in the MO design, which results in in a lower ΔP compared with the BO design. Therefore, since both TMSs in this study provide safe operational temperatures temperatures for LIBs, MO design may be preferred due to its operation with a lower pumping power despite its lower thermal performance compared with the BO design. Minimizing pumping power in practical applications, particularly when a TMS is used for the pack of LIBs in an EV, is substantially beneficial to reduce the overall cost of thermal management.

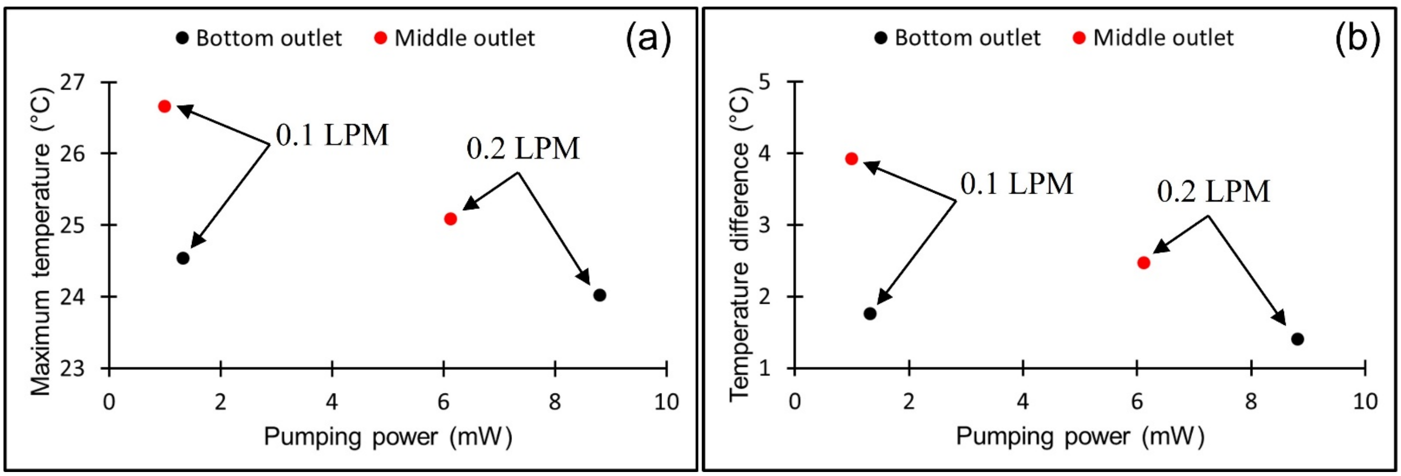

Fig. 2: (a) Maximum cell temperature at different pumping power; (b) temperature difference across the cell at different pumping power.

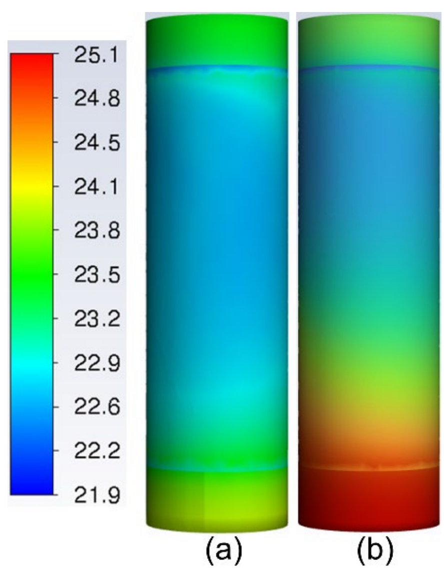

Fig. 3: Temperature distribution on the surface of the LIB cell at the flow rate of 0.2 LPM. (a) BO TMS; (b) MO TMS.

3. Conclusion

Hydrothermal performances of two different TMSs are investigated through three-dimensional simulation of fluid flow and heat transfer inside the TMSs, as well as heat conduction with volumetric heat generation inside a solid volume as representative of a LIB cell. The difference of TMSs is the location of the outlet manifold. It was found that both TMSs provide safe operational temperatures for LIBs, although the BO design has a better thermal performance. This is mainly to the distribution of flow over a larger area from the inlet to the outlet manifold inside the TMS's case in the BO design. However, at a given flow rate, the MO design led to a lower pumping power mainly due to flowing the water through a shorter path from the inlet to the outlet, which resulted in a lower pressure drop in respect to the BO TMS. As a result, depending on design requirements in practical applications, either BO or MO design is useful. If the main objective of the design is maintaining the temperature of LIB cell as low as possible, the BO design is a better option. However, if the main goal of the design is operating the TMS with a minimized pumping power, the MO TMS is an appropriate design.

Acknowledgements

The financial supports from NASA MUREP Institutional Research Opportunity (Award#80NSSC19M0196), the National Science Foundation-CREST Award (Contract #HRD-1914751), and the Department of Energy/National Nuclear Security Agency (DE-FOA-0003945) are gratefully acknowledged.

References

[1] P. Peng, Y. Wang, F. Jiang, "Numerical study of PCM thermal behavior of a novel PCM-heat pipe combined system for Li-ion battery thermal management," *Appl. Therm. Eng.*, vol. 209, p. 118293, 2022.

[2] A. Sarchami, M. Najafi, A. Imam, E. Houshfar, "Experimental study of thermal management system for cylindrical Li-ion battery pack based on nanofluid cooling and copper sheath," *Int. J. Therm. Sci.*, vol. 171, p. 107244, 2022.

[3] M. R. Shaeri, "The key role of pumping power in active cooling systems," in *Proceedings of the 3rd Thermal and Fluids Engineering Conference (TFEC),* Fort Lauderdale, FL, 2018, pp. 1181-1184.

[4] K. Benabdelaziz, B. Lebrouhi, A. Maftah, M. Maaroufi, "Novel external cooling solution for electric vehicle battery pack," *Energy Rep.*, vol. 6, pp. 262-272, 2020.

[5] M. A. Bamdezh, G. R. Molaeimanesh, S. Zanganeh, "Role of foam anisotropy used in the phase-change composite material for the hybrid thermal management system of lithium-ion battery," *J. Energy Storage*, vol. 32, p. 101778, 2020.

[6] M. R. Shaeri, R. Bonner, "Effect of perforation size to perforation spacing on heat transfer in laterally perforated-finned heat sinks," in *Heat Transfer Summer Conference*, 2017, vol. 57892, p. V002T14A005, American Society of Mechanical Engineers.